

Kinetic Isotope Effect in the Gas-Phase Reaction of Muonium with Molecular Oxygen

Ulrich Himmer, Herbert Dilger, and Emil Roduner*

Institut für Physikalische Chemie der Universität Stuttgart, Pfaffenwaldring 55, 70569 Stuttgart, Germany

James J. Pan, Donald J. Arseneau, and Donald G. Fleming

Department of Chemistry and TRIUMF, University of British Columbia, Vancouver, BC, Canada V6T 1Z1

Masayoshi Senba

Department of Physics, Dalhousie University, Halifax, NS, Canada, B3H 3J5

Received: November 13, 1998; In Final Form: January 20, 1999

The rate constant of the gas-phase addition reaction of the light hydrogen isotope muonium to molecular oxygen, $\text{Mu} + \text{O}_2 \rightarrow \text{MuO}_2$, was measured over a range of temperatures from 115 to 463 K at a pressure of 2 bar and from 16 to 301 bar at room temperature, using N_2 as the moderator gas. The reaction remains in the termolecular regime over the entire pressure range. At room temperature, the average low-pressure limiting rate constant is $k_{\text{ch}}^0(\text{Mu}) = (8.0 \pm 2.1) \times 10^{-33} \text{ cm}^6 \text{ s}^{-1}$, a factor of almost 7 below the corresponding rate constant for the $\text{H} + \text{O}_2$ addition reaction, $k_{\text{ch}}^0(\text{H})$. In contrast to $k_{\text{ch}}^0(\text{H})$, which exhibits a clear negative temperature dependence, $k_{\text{ch}}^0(\text{Mu})$ is essentially temperature independent. At room temperature, the kinetic isotope effect (KIE) is strongly pressure (density) dependent and is reversed at pressures near 300 bar. The kinetics are analyzed based on the statistical adiabatic channel model of Troe using a Morse potential, which works well in reproducing the overall KIE. The major factors governing the isotope effect are differences in the moment of inertia and density of vibrational states of the addition complex.

I. Introduction

The largest available mass ratio between conventional isotopes is a factor of 2 between deuterium (D) and protium (H), or a factor of 3 when tritium (T) is included. Over the past two decades, a new isotopic analogue of atomic hydrogen has become important for the investigation of reaction dynamics and kinetic isotope effects (KIEs). It is muonium ($\text{Mu} \equiv \mu^+e^-$), a bound state of a positive muon (μ^+), which takes the role of the nucleus, and an electron. Muonium has a mass only one-ninth that of H but is otherwise chemically identical to H. This remarkable mass ratio leads to unprecedented KIEs in chemical reactions where a bond to the isotope is broken or formed.^{1–3} These primary isotope effects can be 2 orders of magnitude or more, in both directions, depending on the type of reaction. Mu is slower than H when the effect is dominated by the zero-point energy in the transition state, typified by endothermic reactions such as H-abstraction from H_2 ⁴ or CH_4 ,⁵ but it can be considerably faster than H when energy barriers are small and narrow on early-barrier surfaces so that tunneling plays a major role,⁶ typified by exothermic abstraction reactions such as $\text{Mu} + \text{X}_2$,^{7,8} or $\text{Mu} + \text{HX}$,^{9–11} or $\text{Mu} + \text{N}_2\text{O}$ ¹² or addition reactions such as $\text{Mu} + \text{C}_2\text{H}_4$ ^{13,14} or $\text{Mu} + \text{benzene}$.² It is perhaps not surprising that Mu probably holds the world record, with a KIE larger than 75000 at room temperature, in the reaction in which Mu is transferred from the cyclohexadienyl radical to a dimethylbutadiene molecule in solution.¹⁵

It is generally well-known that measurements of chemical reactivity serve as sensitive tests of reaction rate theories and potential energy surfaces (PES). In most studies of this nature, muonium exhibits a primary KIE, but the Mu atom has also

been used as a passive spectator in kinetic studies of radical reactions where the bond to Mu remained intact and where any secondary KIE was undetectable, within error. Such work includes the determination of accurate and absolute rate constants of radical clock reactions such as cyclization and ring fission in the liquid phase¹⁶ and of Mu-ethyl radical addition reactions to O_2 and NO .^{17,18}

Examples of Mu reactivity either concern reactions in liquids or pressure-independent addition reactions to polyatomics in the gas phase, which are in the high-pressure limit at pressures only of order 1 bar,^{13,17,18} due to the large number of degrees of freedom involved. The present study is part of a broad program to investigate Mu reactivity with small molecules, with few degrees of freedom, the H-atom analogues of which have been studied for a number of years¹⁹ and are all of considerable interest in combustion kinetics and atmospheric chemistry.^{20–22} Both Mu and H-atom addition reactions to such small molecule species involve strongly pressure-dependent rates, in contrast to the cases cited above. The addition of Mu to NO has been found to obey low-pressure termolecular kinetics up to 61 bar, where it has been established²³ that Mu is slower than H by a factor of 5 (recently confirmed up to 500 bar), a much more dramatic KIE than had been seen in an earlier D(H) + NO study.²⁴ Current studies of the Mu + CO addition reaction up to 300 bar also reveal pronounced moderator effects.²⁵ The present work investigates Mu addition to oxygen, the chemical analogue of H addition to O_2 , which is of special interest in combustion and flame processes and in atmospheric chemistry^{21,22,26,27} as well as being of considerable current theoretical interest.^{28–37}

In all addition (or “recombination”) studies of this nature, the reaction exothermicity brought to the adduct by the newly formed bond, in this case to the HO₂* complex, has to be transferred in collisions with a third body, usually with an inert moderator gas (M):



The apparent bimolecular rate constant for this reaction, k_{ch} , depends on the moderator concentration [M] and thus on the total pressure. One distinguishes three pressure ranges: (i) the low-pressure regime, where k_{ch} is proportional to [M], $k_{\text{ch}} = k_{\text{ch}}^0[\text{M}]$; (ii) the high-pressure regime, where k_{ch} approaches a constant value, the high-pressure limit k_{ch}^∞ , which in essence is the bimolecular rate constant for the addition step; (iii) the intermediate falloff regime. At quite high temperatures (>1000 K), a second reaction channel becomes important, the bimolecular abstraction reaction,



but this channel is highly endothermic^{38–40} and can be neglected over the temperature range of the present experiment.

The H + O₂ addition reaction, (R1), has been investigated in detail by several groups, over a range of different moderators, pressures, and temperatures,^{19,41–50} and a survey of the results up to 1997 has been reported by Atkinson et al.⁵¹ The most detailed study carried out over a range of high pressures is the work of Cobos et al. In that study, for both Ar and N₂ moderators, the rate constant $k_{\text{ch}}(\text{H})$ approaches about 50% of its high-pressure limit near 200 bar, at room temperature. Investigations of the reaction of D with O₂ in an Ar moderator, in the low-pressure regime, did not reveal any significant isotope effect, $k_0(\text{D})/k_0(\text{H}) \approx 1.52$. For Mu + O₂, one can expect a much stronger KIE, which should prove valuable in refining our understanding of this important combustion reaction. We have therefore investigated the Mu analogue of reaction R1:

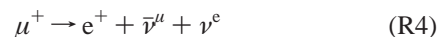


as a function of pressure ($2 \leq p \leq 301$ bar) and temperature ($115 \leq T \leq 463$ K). The temperature dependence studies may also be useful in helping to distinguish between two different functional behaviors which were proposed for H + O₂; Atkinson et al.⁵¹ recommends a T^{-n} dependency, in contrast to the results of Carleton et al.⁵⁰ and Hsu et al.^{48,49} who found that an Arrhenius-like exponential dependency fits their experimental results better. This latter dependence seems to agree well with the earlier data of Kurylo, albeit in a He moderator.⁴¹

II. Experimental Section

a. Muon Spin Relaxation (μSR) Technique in Longitudinal Magnetic Fields. The muon is a spin- $1/2$ particle, like the proton, and is available in beams with a spin polarization close to 100% at the ports of suitable accelerators. Experiments can be carried out in either transverse magnetic field (TF) or longitudinal field (LF) geometries relative to the initial muon polarization in the beam. In a LF experiment, muons are stopped in the target of interest, which is placed in a magnetic field, either parallel or antiparallel to the beam polarization. As a result of its slowing-down processes in the target, the μ^+ finds itself in one of several possible environments at observation times (diamagnetic muons, free muonium, or in a Mu-substituted free radical), with its polarization shared accordingly.¹ Regardless of its environment,

the positive muon decays with a lifetime of 2.2 μs , according to



The decay is parity violating, and the decay positron (detected in the experiments) is consequently emitted preferentially along the instantaneous muon spin direction, at the moment of decay. This effect forms the basis of the time-differential μSR , which monitors the time evolution and relaxation of the muon spin polarization. Details of typical muonium chemistry experiments of this nature have been described elsewhere,^{1,6,53–56} with particular emphasis in the gas phase as well,^{17,23,53} but in short are as follows. Single muons are stopped in the experimental target, and their individual decay times are measured by triggering a clock when a muon enters the target, then stopping the clock when the corresponding decay positron is detected in a scintillation counter, positioned in a fixed direction with respect to the incident muon spin. The present experiments have been carried out in LF, utilizing counters placed in the forward (F) and backward (B) directions. For each counter, positron events are accumulated in a time histogram of the form

$$N(t) = N_B + N_0 e^{-t/\tau_\mu} [1 \pm AP(t)] \quad (1)$$

which represents a modified radioactive decay curve characterized by the muon lifetime τ_μ , a normalization constant N_0 , and a time-independent background N_B . Superimposed is the signal of the relaxing muon polarization, $P(t)$, with its initial amplitude A , which depends on the decay anisotropy, the initial beam polarization, and the solid angle of the detector. (In a TF, $P(t)$ has oscillatory components due to different Larmor precession frequencies, but in a LF, it is in most cases just a relaxing signal). Experiments were carried out at the TRIUMF accelerator in Vancouver, Canada, and at the Paul Scherrer Institute (PSI), near Zürich, in Switzerland. Time histograms were accumulated with a time resolution of about 2.5 ns bin width and a total length of 10 μs .

Three different pressure cells were used at three different accelerator beam ports. (i) Experiments at a pressure of 2 bar were conducted using “surface muons” with a momentum of 29 MeV/c at the πE3 beam line at PSI. The reaction vessel, a stainless steel cylinder of 50 cm length and 8 cm diameter, was placed in the warm bore of a superconducting magnet which reaches fields up to 5 T. The vessel has a 25 μm titanium window, through which the incident muon enters the gas, and is surrounded with a copper tube, which allows the temperature to be regulated by a recirculating liquid (silicone oil for heating and liquid nitrogen for cooling). This vessel was isolated by placing it in a vacuum jacket with a Mylar entrance window. (ii) The intermediate pressure range, up to 61 bar, was also studied with surface muons, in an aluminum gas cell approximately 15.6 cm long with a 9.5 cm inside diameter. The muon beam entered the target cell through a 1.1 cm diameter, 100 μm thick window bored in a 1.1 cm thick titanium end flange. The muon counter was a small disk of plastic scintillator positioned as close to the Ti entrance window as possible, with the whole arrangement attached to the beam line vacuum.⁵⁷ The cell was positioned in the center of a superconducting solenoid operated at magnetic fields from 0.5 to 2 T. These experiments were performed at the TRIUMF M15 surface muon beam port. (iii) For high-pressure experiments, up to 301 bar, we used a stainless steel target vessel, which has a 10 cm length, 5 cm internal diameter and 1.25 cm walls. At one end of the cell, a titanium flange is bolted on and sealed with an O-ring. The

muon entry “window” is a 2.5 cm diameter section of that flange machined to 0.3 cm thickness and a domed shape. Due to the thicker window, we had to use “backward” decay muons, with a momentum around 70 MeV/c at the TRIUMF M9B beam port. The cell was placed in a conventional Helmholtz magnet which reaches fields up to 0.3 T.

At PSI, commercially available oxygen (99.95% stated purity) and nitrogen (99.999%, <2 ppm oxygen) were used without further purification. Both gases were obtained from the Sauerstoffwerk Lenzburg AG. At TRIUMF, all gases were obtained commercially from Canadian Liquid Air. Research grade oxygen (99.997%) and nitrogen (99.9995%, <0.5 ppm oxygen) were used without further purification for pressures up to 61 bar. For higher pressures, research grade nitrogen (99.995%) was further purified by passing through an OxiClear gas purifier (LabClear). The manufacturer’s stated oxygen concentration is below 5 ppb. The density (concentration) was calculated from the measured pressure using the van der Waals equation with constants taken from ref 58.

b. Data Analysis. Each histogram was fitted to the general expression (eq 1) using the nonlinear least-squares fitting program MINUIT.⁵⁹ The main quantity of interest is the polarization, $P(t)$, which relaxes with a characteristic rate (or sum of rates). In addition to the chemical reactions of interest, (R1) and (R3), both (intermolecular) spin exchange (SE) of Mu with paramagnetic O₂ and (intramolecular) spin relaxation (SR) of the MuO₂ radical due to collisions with other molecules can occur, as well as, in principle, SE of MuO₂ with O₂ in addition to SR of the intermediate radical MuO₂^{*}, making for a generally complex kinetics profile.⁶⁰ For the current Mu + O₂ study, there are simplifying assumptions that can be made, discussed below.

We treat the chemical transformation Mu → R as occurring at a chemical rate λ_{ch} . The radical MuO₂ so formed undergoes an intrinsic relaxation upon collisions with other molecules, mostly due to spin-rotation and dipolar interactions, and is therefore dependent on the pressure and the applied magnetic field,^{61,62} whereas Mu is isotropic and does not relax in collisions with an inert moderator. In the presence of oxygen, Mu reacts chemically with the rate λ_{ch} , but it also undergoes spin exchange with the paramagnetic oxygen molecule at a rate λ_{se} . In a LF then, Mu relaxes at a total rate^{17,23}

$$\lambda_{\text{Mu}} = \lambda_{\text{ch}} + \lambda_{\text{se}} = \left(k_{\text{ch}} + \frac{k_{\text{se}}}{2(1+x^2)} \right) [\text{O}_2] \quad (2)$$

where $x = B/B_0$ is the magnetic field in units of the Mu hyperfine field ($B_0 = 0.1585$ T), k_{se} is the bimolecular rate constant for Mu + O₂ SE, and k_{ch} is the chemical rate constant of Mu addition to O₂. In low fields ($x^2 \ll 1$), the SE rate is transmitted to the muon by the hyperfine coupling, but in high fields ($x^2 \gg 1$), the muon is locked to the external field so that the observed relaxation decreases with the decoupling factor $1/(1+x^2)$.^{17,23,63,64} It is assumed that the spin relaxation of the MuO₂ radical, λ_{R} , does not depend on the oxygen concentration since moderator collisions dominate. It can be shown then that the signal of interest, $P(t)$, is given by a double exponential decay:¹⁷

$$P(t) = \frac{\lambda_{\text{se}} - \lambda_{\text{R}}}{\lambda_{\text{Mu}} - \lambda_{\text{R}}} e^{-\lambda_{\text{Mu}}t} + \frac{\lambda_{\text{ch}}}{\lambda_{\text{Mu}} - \lambda_{\text{R}}} e^{-\lambda_{\text{R}}t} \quad (3)$$

Thus, the various contributions to muon spin relaxation have to be separated. The strategy is to determine λ_{Mu} from the dependence on oxygen concentration and to separate the effect

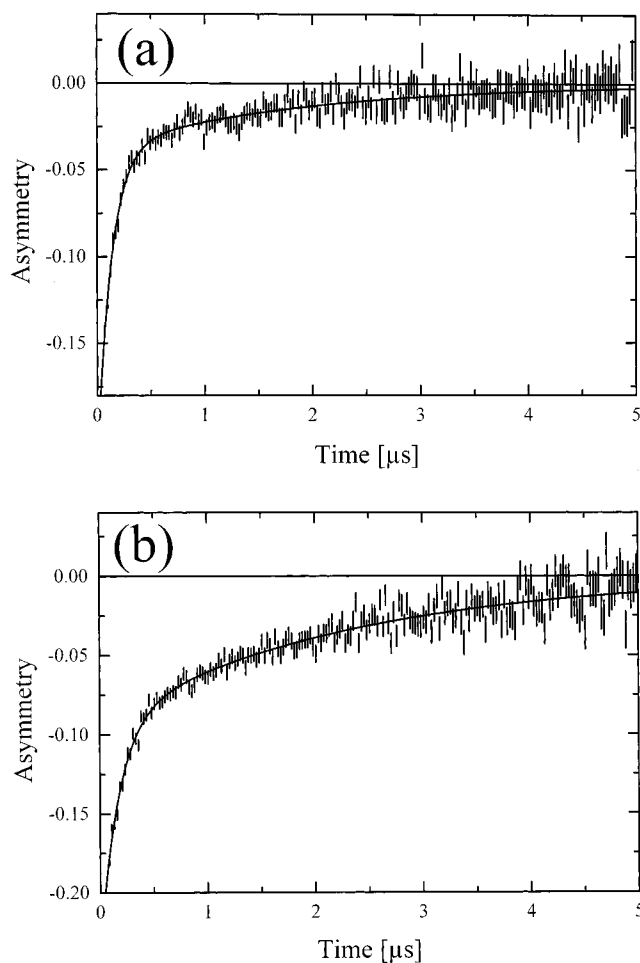


Figure 1. Muon asymmetry measured in forward histograms for Mu + O₂ (+N₂), obtained with the time differential μ SR technique in a longitudinal field at (a) TRIUMF and (b) PSI. The solid lines are double exponential relaxation fits to the data, from which the prime quantity of interest here, λ_{Mu} , is obtained.

of chemical reaction from that due to spin exchange based on the magnetic field dependence of the latter.

There are two principal approximations that go into the expression in eq 3: the MuO₂ (and/or MuO₂^{*}) radical could undergo SE with molecular O₂ and this is neglected; and the SR of the intermediate MuO₂^{*} radical is neglected. In the SE case, the necessary decoupling factor $1/(1+x^2)$ would depend on the much smaller radical hyperfine field, $B_0 \approx 0.0035$ T, estimated from the measured value for the HO₂ radical.⁶⁵ This is so much smaller than that of Mu ($B_0 \approx 0.1585$ T) that, for the fields applied here, any contribution to muon relaxation in the radical due to direct SE is negligible. The second point is in the SR of the intermediate MuO₂^{*} radical, which, as for stable MuO₂ represented by λ_{R} in eq 3, can be expected to depend critically on both applied field and moderator pressure.^{61,66} This dependence can be described by a phenomenological model.⁶¹ Here, the interpretation of λ_{R} does not impact directly on the chemical rate constants of interest and so this aspect will not be discussed further in the present paper.

Figure 1 shows two different experimental histograms, one from TRIUMF at a pressure of 16 bar and a field of 0.7 T and the other from PSI at a field of 3 T and a pressure of 2 bar. Only $AP(t)$ is displayed, and one clearly observes the double exponential nature of the decay. Experimental conditions are chosen such that the fast decay represents λ_{Mu} , the slow one λ_{R} . The principal interest in the present study is λ_{Mu} since this

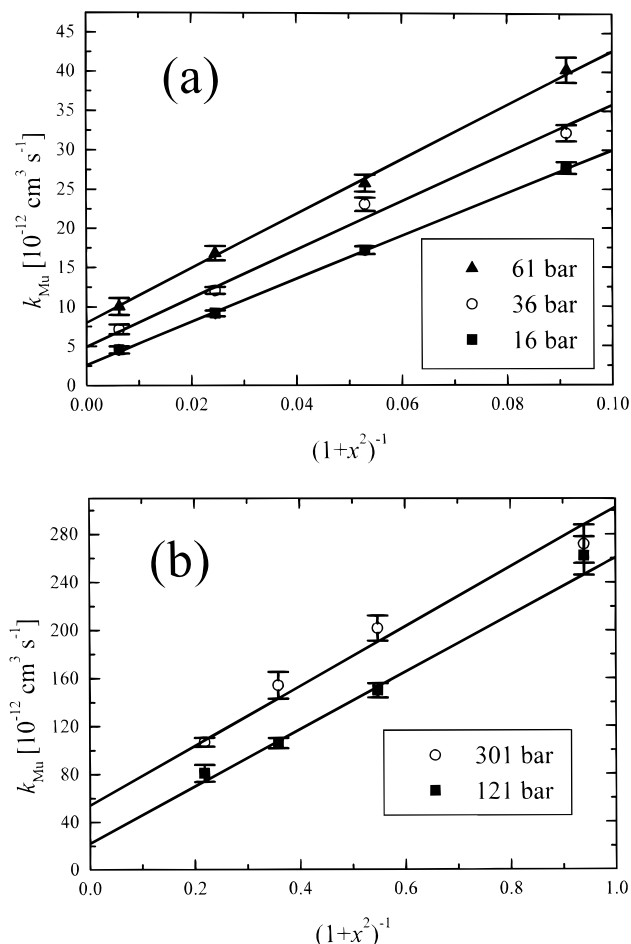


Figure 2. Rate constant of Mu ($k_{\text{Mu}} = \lambda_{\text{Mu}}/[\text{O}_2]$) at ambient temperature in (a) medium-pressure range and (b) higher pressure range plotted against the “quenching” field variable, where $x = B/(1585 \text{ G})$ for muonium. The linear dependence is expected from eq 2, giving the spin-exchange rate constant, $0.5 k_{\text{se}}$, from the slope and the overall chemical rate constant, k_{ch} , from the intercept. (Data from TRIUMF.)

is related to the chemical rate constant, k_{ch} (eq 2). Fitting a single histogram works well as long as λ_{Mu} and λ_{R} are sufficiently different and that the background contributions are sufficiently small. In cases where the separate relaxation rates are not reliably determined from a single histogram, we adopted a procedure in which a set of histograms were fit simultaneously, by choosing a data set which represents different oxygen concentrations but the same magnetic field and total pressure. This allows us to take advantage of the linear dependence of λ_{Mu} on $[\text{O}_2]$ (eq 2) and the fact that λ_{R} is constant in such a set.

III. Results

a. Pressure Dependence. These data were obtained at TRIUMF, at room temperature. One series of experiments was conducted on the M9 beam line with “backward” muons, at 121 and 301 bar N_2 moderator pressures, using the high-pressure cell described above, with several fields in the range between 0.04 and 0.3 T. At these fields and pressures λ_{R} is not that distinct from λ_{Mu} . Moreover, due to scattering of muons into the cell walls as well as scattering of positron contamination in the beam, the μSR signals suffer from a somewhat increased background. We therefore adopted the aforementioned procedure of simultaneously fitting sets of histograms for these data. Another series of runs utilized “surface muons” on the M15 beam line to study the intermediate pressure range (16, 36, and

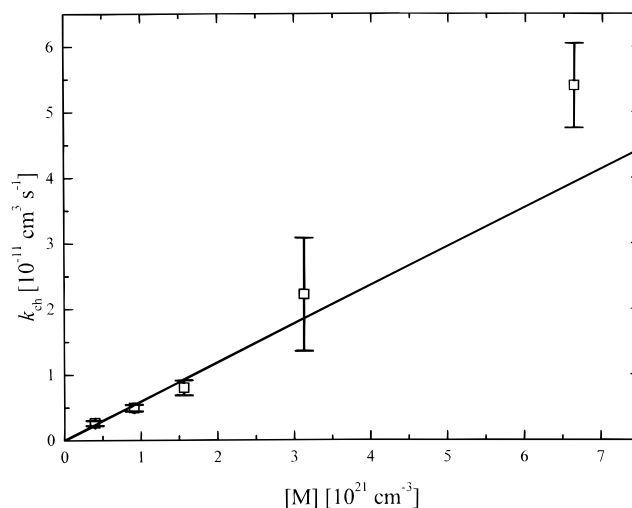


Figure 3. The chemical rate constant at room temperature for $\text{Mu} + \text{O}_2 (+\text{N}_2)$ as found from the intercepts of Figure 2, plotted against the total density, $[\text{M}]$, calculated from the van der Waals equation. The solid line is a linear fit assuming the reaction to be in the low-pressure (termolecular) regime. The departure from the line for the highest density point (301 bar) is not regarded significant (see discussion in the text). The slope of the line yields the termolecular rate constant, $k_{\text{ch}}^0(\text{Mu}) = (5.9 \pm 0.4) \times 10^{-33} \text{ cm}^6 \text{ s}^{-1}$.

61 bar) at fields between 0.5 and 2 T. The conditions here were also such that the most reliable results were obtained by simultaneous fitting of a set of histograms. Figure 2 (parts a and b) displays the results of the global fits in plots of $k_{\text{Mu}} = \lambda_{\text{Mu}}/[\text{O}_2]$ against $1/(1+x^2)$, for different moderator pressures. They clearly demonstrate the linear behavior expected from eq 2. The slopes, which are independent of pressure, correspond to $0.5k_{\text{se}}$, giving an average value $k_{\text{se}} = (5.6 \pm 0.3) \times 10^{-10} \text{ cm}^3 \text{ s}^{-1}$, which is in acceptable agreement with the literature value by Senba et al., $k_{\text{se}} = (5.1 \pm 0.2) \times 10^{-10} \text{ cm}^3 \text{ s}^{-1}$, that was determined by the TF μSR technique at ~ 1 bar moderator pressures⁶⁷ (see also Figure 6). Both the linear dependence on $1/(1+x^2)$, with x specific to the hyperfine field for Mu ($B_0 = 0.1585 \text{ T}$), and the pressure independence of the slopes are consistent with the earlier statement that contributions from SR of MuO_2^* can be neglected.

The k_{ch} values are determined from the intercepts of the plots parts a and b of Figure 2 and are plotted in Figure 3 as a function of the density of nitrogen. There is good linear behavior over the whole pressure range, given the error bars. This indicates that the recombination reaction of Mu with O_2 is in the low-pressure, termolecular regime, where $k_{\text{ch}} = k_{\text{ch}}^0[\text{M}]$, with k_{ch}^0 determined from the slope. The straight line fit gives $k_{\text{ch}}^0(\text{Mu}) = (5.9 \pm 0.4) \times 10^{-33} \text{ cm}^6 \text{ s}^{-1}$.

b. Temperature Dependence. The temperature dependence was measured in the range 115–463 K, using surface muons at PSI, in magnetic fields between 1.4 and 4 T at a total fixed pressure of 2 bar using N_2 moderators. Since the total pressure was much lower than in the TRIUMF data, there was always a clear separation between λ_{Mu} and λ_{R} (e.g., Figure 1b) so that histograms could be fit individually to eq 3. Figure 4 shows the dependence of λ_{Mu} on oxygen concentration at 383 K. The linearity is again expected from eq 2. The slopes increase with decreasing field (decreasing x), because of the increasing effect of spin exchange, which can also be seen from eq 2. The slopes, $k_{\text{Mu}} = \lambda_{\text{Mu}}/[\text{O}_2]$ are plotted in Figure 5 as a function of $1/(1+x^2)$, and good linearity is again obtained, allowing clear separation of k_{ch} and k_{se} . At 383 K, $k_{\text{se}} = (6.2 \pm 0.2) \times 10^{-10} \text{ cm}^3 \text{ s}^{-1}$.

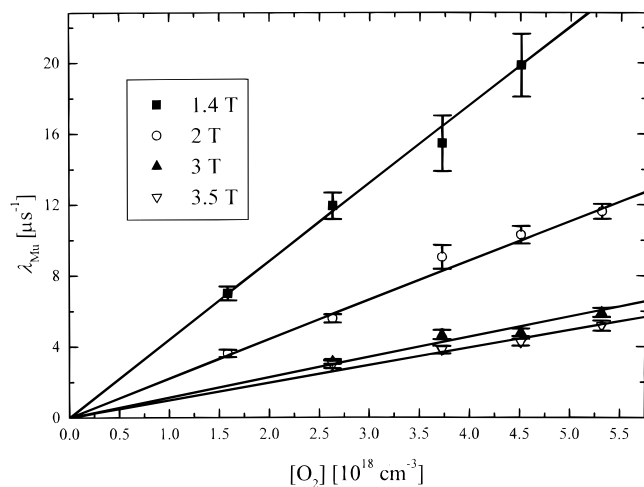


Figure 4. The linear dependence on $[O_2]$ expected from eq 2 for the relaxation rate, λ_{Mu} , for a fixed moderator pressure (2 bar) is demonstrated for four different fields at 383 K. The increasing slope with decreasing field is due to the reduced “quenching” of $Mu + O_2$ spin exchange at lower fields. (Data from PSI.)

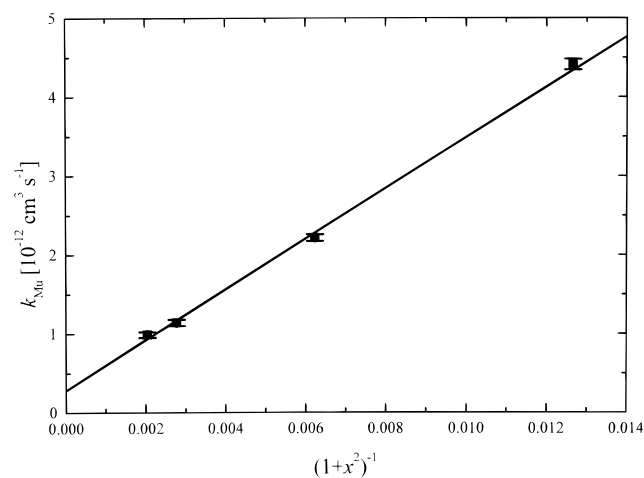


Figure 5. Mu relaxation rate constant found from the slopes of Figure 4 ($k_{Mu} = \lambda_{Mu}/[O_2]$) at 2 bar, 383 K, vs the field variable $1/(1+x^2)$. See caption to Figure 2.

The temperature dependence of the spin exchange rate is given by⁶⁷

$$k_{se}(T) = \sqrt{\frac{8k_B T}{\pi\mu}} \sigma_D(T) \quad (4)$$

where μ is the reduced mass for the relative motion of Mu and O_2 , k_B is Boltzmann’s constant, and $\sigma_D(T)$ is the energy-averaged total SE cross section, the temperature dependence of which becomes apparent only at temperatures less than 100 K.⁶⁷ Thus, if the temperature dependence of $\sigma_D(T)$ is weak enough (often approximated as a temperature-independent hard-sphere value), $k_{se}(T)$ should follow $T^{1/2}$ over the temperature range of the present study. Figure 6 compares the values of $k_{se}(T)$ from the present experiments with those of the TF measurements of ref 67. Though there is some scatter, the individual values generally agree within errors. A good fit to the data (open squares in Figure 6) is found for an assumed $T^{1/2}$ dependence, giving $k_{se}(T) = ((3.16 \pm 0.05) \times 10^{-11})T^{1/2} \text{ cm}^3 \text{ s}^{-1}$. Recent theoretical calculations of the SE cross section for $H + O_2$ suggest a weak temperature dependence of $\sigma_D(T) \sim (295/T)^{1/3}$.⁶⁸ Although this same dependence does not have to apply to the analogue Mu

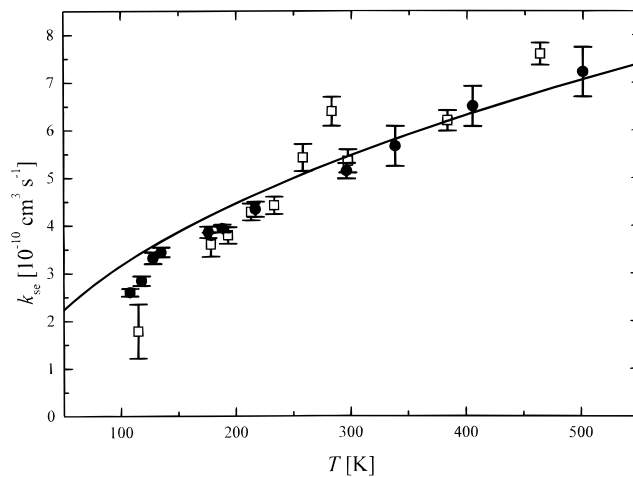


Figure 6. Temperature dependence of the spin exchange rate constant k_{se} , compared with the earlier data of Senba et al. obtained with a transverse field ?SR technique;⁶⁷ open squares, this work; closed circles, ref 67. Note the generally good level of reproducibility. The line is a fit of a $T^{1/2}$ dependence to the data of this work.

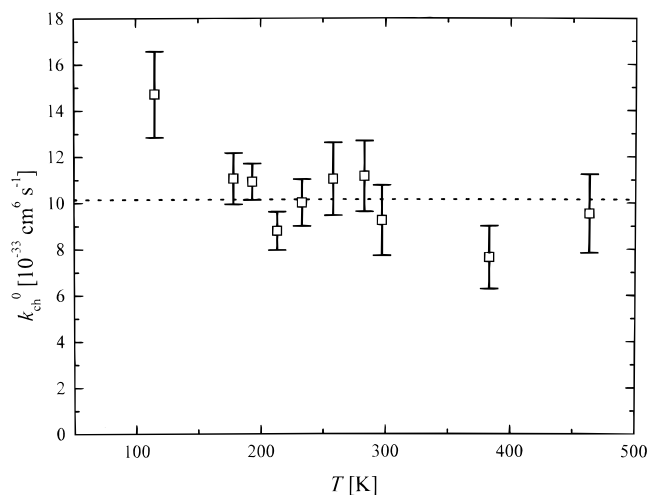


Figure 7. Temperature dependence of the termolecular rate constant for $Mu + O_2$, $k_{ch}^0(Mu)$, measured at a moderator pressure of 2 bar. With the possible exception of the point at 115 K, the rate constants are independent of temperature (see Figure 9). (Data from PSI.)

reaction (the SE cross sections for $Mu + O_2$ are considerably smaller than for $H + O_2$),^{64,67} Figure 6 reveals a clear trend of increasing σ_D with T .

Since the low-pressure regime extends up to 301 bar (Figure 3), at 2 bar one can plot directly $k_{ch}^0 = k_{ch}/[M]$, instead of k_{ch} , as a function of temperature, as shown in Figure 7. The data are clearly consistent with little or no dependence on temperature, in contrast to the much stronger decrease with increasing temperature seen in the corresponding $H + O_2$ data^{48–50} in N_2 moderator, which can be fit with a negative activation energy of about -6 kJ/mol . Assuming no temperature dependence, a fit of the Mu data gives, $k_{ch}^0(Mu) = (10.1 \pm 0.4) \times 10^{-33} \text{ cm}^6 \text{ s}^{-1}$. This value is significantly higher than that reported above, obtained from the range of pressure measurements done at TRIUMF, $k_{ch}^0(Mu) = (5.9 \pm 0.4) \times 10^{-33} \text{ cm}^6 \text{ s}^{-1}$. This systematic error which is discussed further in section IV is accounted for by a weighted average: $k_{ch}^0(Mu) = (8.0 \pm 2.1) \times 10^{-33} \text{ cm}^6 \text{ s}^{-1}$. Interestingly, this result is almost the same as that reported in N_2 moderator for the $Mu + NO$ addition reaction up to 61 bar pressure,²³ $k_{ch}^0(Mu + NO) = (8.8 \pm 0.5) \times 10^{-33} \text{ cm}^6 \text{ s}^{-1}$.

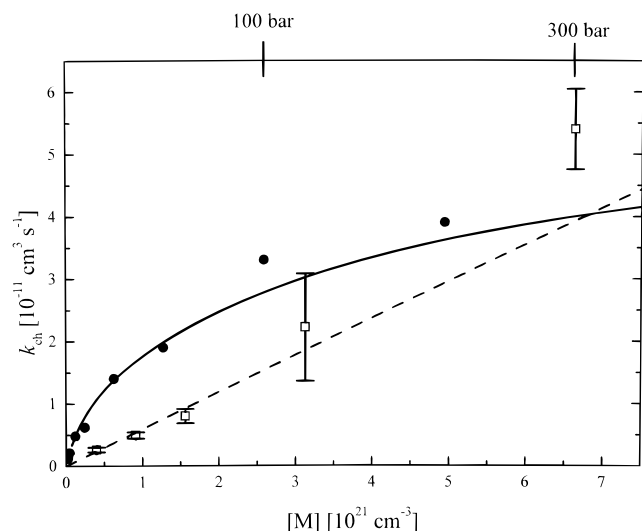


Figure 8. Dependence of the chemical rate constant on moderator (N_2) density: Open squares, $Mu + O_2 (+N_2)$, this work; the dashed line is a fit to the assumed linear dependence; closed circles, $H + O_2 (+N_2)$, errors 30%.⁴⁶ The solid line is calculated from eq 17, using the parameters given in ref 46.

TABLE 1: Literature Values for the Low-Pressure Rate Constant at Room Temperature for the Reaction $H + O_2 (+N_2)$

study	$k_{ch}^0(H)$ [$10^{-33} \text{ cm}^6 \text{ s}^{-1}$]
Kurylo, 1972 ⁴¹	53 ± 8
Cobos et al., 1985 ⁴⁶	65 ± 10
Wong and Davis, 1974 ⁴²	55 ± 7
Hsu et al., 1987 ⁴⁹	60 ± 9
Carleton et al., 1993 ⁵⁰	46 ± 3
Baulch et al., 1992 ⁶⁹	40 ± 20
Atkinson et al., 1997 ⁵¹	54 ± 11

IV. Discussion and Theory

The current results for the measured pressure dependence in the rate constant for the $Mu + O_2$ reaction are summarized and compared with a corresponding study by Cobos et al.⁴⁶ for the $H + O_2$ reaction in Figure 8. While Mu is obviously slower and in the low-pressure linear range up to the highest densities measured, the clear curvature in the $H + O_2$ data demonstrates that the latter reaction is already in the falloff regime at densities of $0.5 \times 10^{21} \text{ cm}^{-3}$, or at pressures of only about 25 bar. As a result, the KIE is clearly pressure dependent, approaching unity near 300 bar. The limiting slope of the $H + O_2$ data is $k_{ch}^0(H) = (65 \pm 10) \times 10^{-33} \text{ cm}^6 \text{ s}^{-1}$, as reported in ref 46, which is in good agreement with other room-temperature H-atom data, as summarized in Table 1. The average of these cited values agrees with the 1997 recommended value of Atkinson et al., $k_{ch}^0(H) = (55 \pm 11) \times 10^{-33} \text{ cm}^6 \text{ s}^{-1}$,⁵¹ which shall be taken for comparison with the present $Mu + O_2$ data. The KIE at room temperature in N_2 moderator is then $k_{ch}^0(Mu)/k_{ch}^0(H) = (8.0 \pm 2.1)/(55 \pm 11) = (0.15 \pm 0.05)$. This result is similar to the KIE reported in a comparison of $H + NO$ and $Mu + NO$ addition rate constants, (0.23 ± 0.12) .²³

Several of the $H + O_2$ measurements have also been carried out in Ar moderator.^{46,48–50} The corresponding termolecular rate constant recommended by Baulch et al.⁶⁹ is $(18 \pm 9) \times 10^{-33} \text{ cm}^6 \text{ s}^{-1}$ at room temperature. This can be compared with the measurements of the $D + O_2$ reaction in Ar moderator,⁵² $k_{ch}^0(D) = (17 \pm 1) \times 10^{-33} \text{ cm}^6 \text{ s}^{-1}$, for a KIE = $k_{ch}^0(H)/k_{ch}^0(D)$ of essentially unity, reinforcing our earlier statement of the importance of Mu reactivity to understanding kinetic isotope effects in unimolecular kinetics.

In the following, we shall discuss our results, in comparison with those for $H + O_2$, based on the theoretical framework of unimolecular kinetics developed by Troe,^{70–78} which facilitates a transparent breakdown of the total kinetic isotope effect into its different contributions. Comparison is also made with the transition state theory (TST) calculations of Duchovic and co-workers.³⁶ Troe's treatment is first developed for the reverse process, the unimolecular decay, which in this context is the reverse of (R3 or R1), rewritten here as



with the rate constant for the recombination process (R3) related to the unimolecular dissociation process (R5) by^{79,80}

$$k_{ch}(=k_{rec}) = k_{uni}K_{eq} \quad (5)$$

where K_{eq} is the equilibrium constant for overall recombination/addition (R1, R3) that is calculated from statistical thermodynamics. For the Mu reaction, it has the usual form

$$K_{eq} = \frac{Q_{el}^{MuO_2} Q_{vibrot}^{MuO_2}}{Q_{el}^{Mu} Q_{el}^{O_2} Q_{vibrot}^{O_2} Q_{trans}^{Mu+O_2}} e^{-\Delta H_0^0/k_B T} \quad (6)$$

where ΔH_0^0 is the reaction enthalpy for recombination at 0 K ($-3.35 \times 10^{-19} \text{ J}$ for $H + O_2$ and $-2.47 \times 10^{-19} \text{ J}$ for $Mu + O_2$), and the Q_i^x are the partition functions for the i -th degree of freedom of species x . Following Troe, we now treat the low-pressure and high-pressure regimes separately.

a. Low-Pressure Regime. In the low-pressure range, the unimolecular rate constant is^{70–72}

$$k_{uni}^0 = k_{uni}^{0,SC} \beta_c \quad (7)$$

where $k_{uni}^{0,SC}$ is the rate constant in the strong collision limit and deviations from it are described by the "weak collision" efficiency factor $0 \leq \beta_c \leq 1$. The latter depends on the average collisional energy transfer, $\langle \Delta E \rangle$, which is difficult to calculate and so is normally treated empirically. It was found in early studies that β_c depends more on the properties of the moderator than on those of the reaction partners,⁷² though it clearly depends as well on the number of degrees of freedom with its interpretation depending on the method of analysis.⁸¹ To our knowledge, no explicit isotopic dependence has been reported to date, but since β_c depends directly on $\langle \Delta E \rangle$ and since the level density in MuO_2^* is considerably less than in HO_2^* , with a concomitant increase in $\langle \Delta E \rangle$, β_c depends at least implicitly on isotopic mass. Nevertheless, as a first approximation, we shall assume

$$\beta_c(Mu) \approx \beta_c(H) \quad (8)$$

At room temperature, Cobos et al.⁴⁶ find $\beta_c(H) \approx 0.29$. Thus, in the estimation of KIEs, the main factor to be considered is $k_{uni}^{0,SC}$, which can be broken down in the following way:^{71,72}

$$k_{uni}^{0,SC} = Z_{LJ} \int_0^\infty dJ \int_{E_0(J)}^\infty f(E, J) dE = Z_{LJ} \frac{\rho_{vib,h}(E_0) k_B T}{Q_{vib}^{H/MuO_2}} e^{-E_0/k_B T} F_{anh} F_E F_{rot} \quad (9)$$

where Z_{LJ} is the Lennard-Jones collisional rate and E_0 is the threshold energy for dissociation, including zero-point-energy (ZPE) in the dissociating ($H-O_2$) bond. As a first approximation, one assumes nonrotating molecules consisting of harmonic

TABLE 2: Contributions to the Kinetic Isotope Effect in the Low-Pressure Limit

term	H	Mu	ratio Mu/H
Z_{LJ} [$10^{-16} \text{ m}^3 \text{ s}^{-1}$]	3.74	3.76	1.01
$\rho_{\text{vib,h}}(E_0)$ [10^{20} J^{-1}]	19.8	2.29	0.12
\tilde{K}_{eq} [10^{-30} m^3]	6.12	50.2	8.20
F_{anh}	1.78	1.78	1.00
F_E	1.02	1.02	1.00
F_{rot}	6.12	4.93	0.81
$\exp(-\Delta E_Z^0/k_B T)$	0.89	0.49	0.54
k_{ch}^0 [$10^{-33} \text{ cm}^6 \text{ s}^{-1}$]	53.4	22.4	0.42

oscillators with an energy-independent density of H/MuO₂ states $\rho_{\text{vib,h}}$. The F factors, as given in Table 2, are corrections for anharmonicity (F_{anh}), energy dependence of density of states (F_E), and rotational effects (F_{rot}). Since the only barrier for the addition reaction is the zero-point energy barrier, ΔE_Z^0 , as a result of disappearing oscillators in the reaction channel, one has

$$E_0 = -\Delta H_0^0 + \Delta E_Z^0 \quad (10)$$

In defining

$$\tilde{K}_{\text{eq}} = K_{\text{eq}} \exp(\Delta H_0^0/k_B T) \quad (11)$$

one ends up in

$$k_{\text{rec}}^0 = \beta_c \tilde{K}_{\text{eq}} Z_{LJ} \frac{\rho_{\text{vib,h}}(E_0) k_B T}{Q_{\text{vib}}^{\text{H/MuO}_2}} F_{\text{anh}} F_E F_{\text{rot}} e^{-\Delta E_Z^0/k_B T} \quad (12)$$

Following the procedure outlined in refs 71 and 72, all these factors have been calculated separately for the Mu + O₂ and the H + O₂ reactions. The potential surface is approximated by a Morse potential in the direction of the reaction coordinate (Morse parameter β) and by a “loosening parameter” α describing the decrease of the ZPEs of the two oscillators perpendicular to the reaction coordinate, as the reaction proceeds. Neither of the parameters α or β are expected to be influenced by isotope effects, so the values for MuO₂ were taken to be the same as those of HO₂, from the results of Cobos et al.,⁴⁶ $\beta = 2.94 \times 10^{10} \text{ m}^{-1}$ and $\alpha = 0.94 \times 10^{10} \text{ m}^{-1}$. The geometry as well as the normal-mode frequencies and ZPEs of HO₂ and MuO₂ were obtained from literature⁴⁶ or calculated using the “Turbomole” program⁸² with the density functional method BLYP.^{83,84} The results, given as separate contributions to the overall KIE, are collated in Table 2.

The first entry in this table is the collisional rate of MuO₂/HO₂ with N₂ moderator and gives little or no contribution since the collision partners have essentially equal masses. The second entry is the (energy-independent) harmonic density of states which is markedly less for the Mu analogue due to the increased $\nu_r(\text{Mu})$. The third entry is for \tilde{K}_{eq} , which enhances the reaction of Mu over that of H by a factor of 8.2. The large ratio of isotopic masses affects both the translational and the rotational partition functions. The effect on the former gives a factor of 25, which is partially compensated by the effect on the latter. All the other factors favor the H reaction. The most important effects are from the lower density of states for the MuO₂ molecule and the enhanced \tilde{K}_{eq} for the Mu reaction. The overall contributions then yield a room-temperature KIE in the low-pressure regime

$$k_{\text{ch}}^0(\text{Mu})/k_{\text{ch}}^0(\text{H}) = 0.42 \quad (13)$$

Comparing this value with the experimental KIE, 0.15 ± 0.05 ,

the trend is qualitatively reproduced. The quantitative discrepancy can be traced, in part, to the simplifying assumptions adopted here about the potential energy surfaces, but the basis of the theoretical model of Troe employed here, despite its well recognized success, also needs to be critically assessed in terms of the unusual sensitivity to KIEs brought to light by studies of the Mu atom. Several areas for further reflection suggest themselves.

(i) The theory implicitly assumes the validity of the Born–Oppenheimer (BO) approximation. Although much lighter than the proton, the muon is nevertheless 200 times heavier than the electron. A quantitative treatment is difficult, but earlier estimates indicate that deviations from BO should be relatively constant (although in absolute terms not negligible) as long as the electron population on the muon (proton) does not change appreciably over the reaction path and as long as there is no avoided crossing of electronic states that influences the energy along the reaction coordinate.^{4,85}

(ii) The question as to the nature of the PES itself is a critical one. As is standard in most applications of the Troe theory, the present calculation has assumed a Morse potential in concert with the “loosening parameter” α , and it has previously been established that phenomenological choices of this nature can give quite different results.⁴⁶ (A smaller value of α actually describes the experimental KIE effect better.) There have been several recent ab initio surfaces reported for the H + O₂ reaction,^{68,86–90} all of which would be considerably more accurate than the Morse potential used here. There is a small barrier in the Walch et al. surface ($\sim 0.5 \text{ kJ/mol}$)^{87–89} but no barrier in the surface of Pastrana et al.⁸⁹ which seems to be the consensus result of most experiments, in contrast to the earlier surface of Melius and Blint,⁹¹ now recognized as having too high a barrier ($\sim 10 \text{ kJ/mol}$).^{37,86–88} The Walch surface has been used in the TST/RRKM calculations of reaction (R1) by Duchovic et al.,³⁷ which are discussed briefly below. The “DMBE IV” surface of ref 89 has been used in a number of recent rigorous quantum calculations for reaction (R1)^{28–34} as well for the endothermic abstraction reaction, (R2).^{92–95} In the present context, this analytic surface⁸⁹ could be fit to a Morse-type potential, while maintaining the Troe theoretical framework, and this modification is now underway⁹⁶ and is expected to discriminate between the effects of the basic assumptions and those of a not sufficiently accurate PES.

(iii) The question of the suitability of the assumption of chemical equilibrium for MuO₂ for which quantum effects are much more important than in the absence of Mu needs to be critically assessed. Resonant states could well play a crucial role in the case of the MuO₂^{*}, since the density of states will be much lower than for HO₂^{*} (recall Table 2). The dissociation of HO₂^{*} is already non-RRKM,^{31,32,97} and while the average lifetime of these states does follow an RRKM model, there are large quantum fluctuations, which can be expected to be exacerbated in the case of MuO₂^{*}. This could have a greater impact at higher pressures, toward the high-pressure limit, where energy randomization plays a more important role than collisional energy transfer in statistical theories such as RRKM or the Troe theory.

(iv) The degree of collisional energy transfer depends on the density of states, and the first-order assumption made of a mass-independent collision efficiency β_c (eq 8) is probably not justified for mass ratios as large as the factor of 9 prevailing between H and Mu. This question of isotopic effects on collisional energy transfer raised by the present paper is an important one, since there are no other comparisons that are

sensitive enough to make a critical test. Earlier work on comparing D/H isotope effects in vibrational deactivation of large molecules⁹⁸ has emphasized the relative importance of quantum effects in the H-atom species (which would of course be much greater for Mu). Recent work on the kinetics of CH(D) in collisions with light molecules has also emphasized the importance of density of state effects,⁹⁹ but to our knowledge, there are no specifically relevant experiments of isotope effects on energy transfer for the small molecule system of interest here. A number of current models include as well the effects of anharmonicity,^{71,72,77} and the different effects of these models are currently being evaluated.⁹⁶ It may also be that nonadiabatic effects¹⁰⁰ play an important role in collisional energy transfer, in addition to possible electronic nonadiabatic effects arising from the PES.^{68,86–88}

(v) Only two of the three vibrational modes ($\tilde{\nu}_{\text{O-O}} = 1098 \text{ cm}^{-1}$ and $\tilde{\nu}_{\text{bending}} = 1392 \text{ cm}^{-1}$) of excited HO₂ can be deexcited efficiently by collisional energy transfer.¹⁰¹ The highest H–O stretching mode can hardly contribute as a consequence of its high frequency ($\tilde{\nu}_{\text{H-O}} = 3436 \text{ cm}^{-1}$). For MuO₂, the frequencies are $\tilde{\nu}_{\text{Mu-O}} = 9775 \text{ cm}^{-1}$, $\tilde{\nu}_{\text{O-O}} = 1082 \text{ cm}^{-1}$, and $\tilde{\nu}_{\text{bending}} = 3819 \text{ cm}^{-1}$. This means that only the O–O stretching mode might remain to contribute to the collision efficiency. So, when the effective vibrational modes are reduced from two (HO₂) to one (MuO₂), one might estimate $\beta_{\text{c}}(\text{MuO}_2) = 1/2\beta_{\text{c}}(\text{HO}_2)$.¹⁰²

(vi) Though quantum effects are included in both the threshold energies and in the vibrational partition functions, the Troe theory remains a semiclassical one. Tunneling is neglected but could also contribute to $k_{\text{ch}}(\text{Mu})$. Since current PESs indicate little or no electronic barrier, it is likely that the (broad) centrifugal barrier determines tunneling. Simplistically, one would expect this to raise the contribution from F_{rot} for the Mu reaction, thereby raising the theoretical KIE and hence worsening the agreement with experiment.

A first principles calculation, utilizing the accurate ab initio PES of Walch et al.^{86–88} and conventional TST/RRKM theory, has recently been reported by Duchovic et al., in calculations of (R1) and its deuterium analogue,^{36,37} over the whole pressure range leading up to the high pressure limit. Since the mass ratio between H and D is only a factor of 2, the neglect of tunneling is not a serious omission. Though the calculated high-pressure limit is about a factor of 4 below the experimental results of Cobos et al.,⁴⁶ which may be partly explained by the fact that the Walch surface does have a small electronic barrier, the overall level of agreement between experiment and theory is quite good. Not commented upon by the authors is the fact that their calculated KIE, $k_{\text{ch}}^0(\text{H})/k_{\text{ch}}^0(\text{D})$, is of order unity, in accord with the experimental result.⁵² It would be of considerable interest to have this calculation repeated for the present Mu + O₂ data, to assess the importance of tunneling.

It is also of interest here to compare the present result for Mu + O₂ (+ N₂), with that of the similar reaction Mu + NO (+N₂).²³ It is curious that these rate constants are virtually the same, as is the KIE, $k_{\text{ch}}^0(\text{Mu} + \text{NO})/k_{\text{ch}}^0(\text{H} + \text{NO}) = 0.2$. This level of agreement, while perhaps fortuitous, seems to suggest similar chemical reaction mechanisms in both reactions. Both the H + NO^{103,104} and H + O₂^{86–89} PESs have essentially no electronic barrier, and the bond dissociation energies are similar as well. More recent studies of the Mu + NO recombination kinetics, for different moderators, up to pressures of 500 bar,¹⁰⁵ have confirmed the KIE of 0.2. Both these NO studies and the present Mu + O₂ work provide unique data sets which call for calculations, along the lines of those reported in refs 30–32, 35–37, to provide stringent tests for current theoretical models.

b. High-Pressure Limit and Falloff Regime. The high-pressure limit in statistical approaches to recombination kinetics gives the rate constant for the addition step and can be written in the general form

$$k_{\text{ch}}^{\infty} = \frac{k_{\text{B}}T}{h} \frac{Q^{\#}}{Q} e^{-E_0/k_{\text{B}}T} K_{\text{eq}} \quad (14)$$

where $Q^{\#}$ is a pseudopartition function of the activated complex. From the form of eq 14 and the equilibrium constant of eq 6, the limiting high-pressure rate constant for the recombination reaction (R3) can be written in the simplified version of the SACM of Troe and co-workers:^{72,73,106}

$$k_{\text{ch}}^{\infty} = \frac{k_{\text{B}}T}{h} \left(\frac{h^2}{2\pi\mu k_{\text{B}}T} \right)^{3/2} \frac{Q_{\text{el}}^{\text{MuO}_2}}{Q_{\text{el}}^{\text{Mu}} Q_{\text{el}}^{\text{O}_2}} \frac{Q_{\text{cent}}^* F_{\text{AM}}^*}{Q_{\text{vibrot}}^{\text{O}_2} \sigma^*} \prod_r Q_j^* \prod_b Q_m^* e^{-\Delta E_{\text{Z}^0}/k_{\text{B}}T} \quad (15)$$

The Q_j^* are the partition functions of the oscillators in the activated complex. Several of the factors in eq 15 depend on the parameters α and β which have been determined by Cobos et al. in fitting eq 15 to the experimental data to give the value $k_{\text{ch}}^{\infty}(\text{H}) = 7.5 \times 10^{-11} \text{ cm}^3 \text{ s}^{-1}$.^{46,106} For the Mu reaction using the same parameters for α and β we obtain $k_{\text{ch}}^{\infty}(\text{Mu}) = 1.4 \times 10^{-10} \text{ cm}^3 \text{ s}^{-1}$ and a calculated KIE, $k_{\text{ch}}^{\infty}(\text{Mu})/k_{\text{ch}}^{\infty}(\text{H}) \approx 1.9$, in the high-pressure limit.

Unfortunately, the value of $k_{\text{ch}}^{\infty}(\text{H})$, obtained by extrapolation of the falloff curves of refs 46 and 106 has to be directly verified by experiment, since the pressures required to actually reach the high-pressure limit are >2000 bar for H + O₂.⁴⁶ This pressure is expected to be even higher for the Mu + O₂ reaction, putting it out of the range of the μSR technique. Determinations of $k_{\text{ch}}^{\infty}(\text{Mu})$ have been reported for organic polyatomics, where the high-pressure limits are achieved at much lower pressures, of order 1 bar, due to the large numbers of rovibrational degrees of freedom accessed.^{2,13} Interestingly, these rate constants are much smaller than the estimate for $k_{\text{ch}}^{\infty}(\text{Mu})$ above; for example, in the Mu + C₂H₄ reaction, $k_{\text{ch}}^{\infty}(\text{Mu}) = 6.6 \times 10^{-12} \text{ cm}^3 \text{ s}^{-1}$, almost a factor of 100 smaller.

Another perspective on the high-pressure KIEs is provided by the aforementioned TST/RRKM calculations of Duchovic et al.^{36,37} These authors have also calculated k_{ch}^{∞} for the H(D) + O₂ reactions and, while their absolute value for $k_{\text{ch}}^{\infty}(\text{H}) = 2 \times 10^{-11} \text{ cm}^3 \text{ s}^{-1}$ falls below the experimental value reported by Cobos et al.,⁴⁶ the ratio $k_{\text{ch}}^{\infty}(\text{H})/k_{\text{ch}}^{\infty}(\text{D})$ equals 1.4 over a range of temperatures, almost exactly what one would expect from a classical mean velocity dependence. In comparisons of H + C₂H₄ and Mu + C₂H₄, cited in ref 13, the KIE $k_{\text{ch}}^{\infty}(\text{Mu})/k_{\text{ch}}^{\infty}(\text{H}) \approx 3$ at the highest temperatures, about 500 K, was also consistent with this kind of dependence. In the present study at room temperature, $k_{\text{ch}}^{\infty}(\text{Mu})/k_{\text{ch}}^{\infty}(\text{H}) = 1.9$ is less than this ratio, but not all that different. The main isotopic effect in k_{ch}^{∞} for H + O₂ and Mu + O₂ from eq 15 comes from the translational partition functions, the factor of 25 that favors the Mu reaction and the Q_j^* and the factor $e^{-\Delta E_{\text{Z}^0}/k_{\text{B}}T}$ which disfavors the H reaction by 0.54 (Table 2).

The pressure dependence in the falloff regime for the H reaction plotted in Figure 8 is also of interest and can be described by the reduced falloff curves developed by Troe.^{73,74} These have their basis in the ‘‘Lindemann–Hinshelwood’’ form

$$F_{\text{LH}} = \frac{k_{\text{ch}}}{k_{\text{ch}}^{\infty}} = \frac{k_{\text{ch}}^0[\text{M}]}{k_{\text{ch}}^{\infty} + k_{\text{ch}}^0[\text{M}]} \quad (16)$$

Troe has adopted this ratio along with guidance from reduced Kassel integrals, which can be written in a similar form,⁷⁴ in terms of two parameters, F_{cent} and N ,^{73,74}

$$\log(k_{\text{ch}}/k_{\text{ch}}^{\infty}) \cong \log\left(\frac{k_{\text{ch}}^0[\text{M}]}{k_{\text{ch}}^{\infty} + k_{\text{ch}}^0[\text{M}]}\right) + \frac{\log F_{\text{cent}}}{1 + [\log(k_{\text{ch}}^0[\text{M}]/k_{\text{ch}}^{\infty})/N]^2} \quad (17)$$

The parameter F_{cent} is a “broadening factor”, to account for the difference from the simpler Kassel integral, and is actually a product of distributions for weak and strong collision effects of similar (Gaussian) form, and N corresponds to the width of this distribution.⁷⁴ As written, eq 17 is for higher temperatures; at lower temperatures, the distribution is more sharply peaked. Although the approach is somewhat simplified, the beauty of eq 17 is that it allows a good estimate of the pressure dependence of the rate constants without recourse to more rigorous calculations, which are difficult to carry out between the limits of low and high pressures. By fitting the form of eq 17 to experimental data, if k_{ch}^0 is known, the experimental value of k_{ch}^{∞} can be found, provided that there is a sufficient range of pressures measured over which clear curvature is established. This is the case for the H + O₂ reaction and is the procedure that has been used to find $k_{\text{ch}}^{\infty}(\text{H})$ from experimental data,⁴⁶ as given by the solid line in Figure 8. However, this is not possible for the Mu + O₂ reaction, which shows no credible curvature up to the highest pressures measured (see also Figure 3). In this context it can be commented that an alternate approach to the use of reduced falloff curves, based strictly on RRKM behavior, has been given recently by Prezhdo,¹⁰⁷ and his curves and those of Troe are reasonably similar at moderately high temperatures, at least for the recombination of CH₃ radicals considered.

Following the procedure outlined in ref 75 both F_{cent} and N have been calculated for reactions (R1) and (R3), which as it turns out, are about the same. Hence, a similar pressure dependence is expected for both reactions; in particular, they should both show deviation from the low-pressure limit in the pressure range under investigation. The experimental observations (Figure 8) clearly contradict this expectation. There are a number of possible reasons that could explain this contradiction. One is certainly that the approach of utilizing reduced falloff curves, despite the inherent appeal in its approach, is just too simplified, and specific non-RRKM mass and/or angular momentum effects are playing more important roles than the Troe formalism accounts for. We have commented on this aspect above as well, in connection with calculations of k_{ch}^0 . It would be interesting in this respect to have a comparison of Mu + O₂ and H + O₂ from the recent RRKM calculations of Prezhdo.¹⁰⁷ Another aspect is the role played by tunneling, which is not included in the inherently classical formalism of Troe (or Prezhdo). It may be that tunneling effects, much more facile for Mu than H, are strongly pressure dependent, which could also have an impact on fitted temperature dependences over different pressure ranges. If tunneling is significant, both the addition and the dissociation processes could be greatly enhanced with the effect that the range of the low pressure regime could be significantly expanded, which is not inconsistent with the experimental findings.

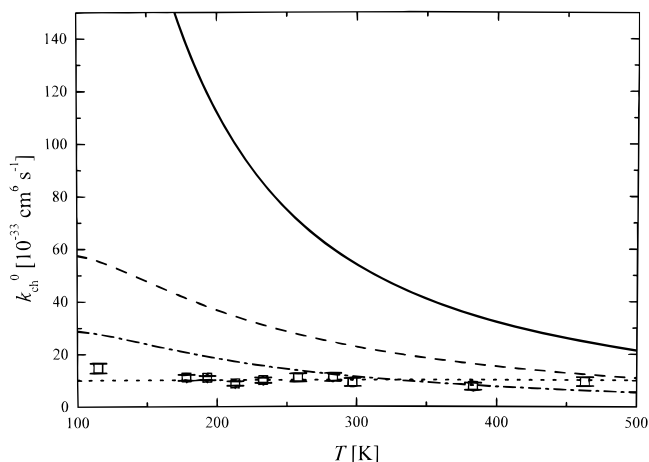


Figure 9. Comparison of the temperature dependence of the chemical rate constants for H + O₂ and Mu + O₂ from the present study at 2 bar (open squares). The solid line is the recommended $T^{-1.8}$ dependence for several H + O₂ experiments by Atkinson et al.⁵¹ The dotted line assumes no temperature dependence and is a fit to the data points. The dashed line is calculated from the Troe theory for the Mu + O₂ by multiplying the recommended value of ref 51 with the calculated KIE assuming $\beta_c(\text{Mu}) = \beta_c(\text{H})$. Same for the dash-dotted line, but assuming $\beta_c(\text{Mu}) = 1/2\beta_c(\text{H})$. (See discussion in the text.)

c. Temperature Dependence. Gas-phase recombination reactions of the radical-radical type typically have little or no electronic barrier, with rate constants that tend to follow a T^{-n} dependence, rather than the traditional Arrhenius law.^{51,109} It can be argued that such a T^{-n} relation is more compatible with theory,¹⁰⁹ but it is still empirical in form, like the Arrhenius law itself. In fact, often combinations of T^{-n} and Arrhenius dependences are employed in order to fit experimental data.^{81,108,109}

There have been two experimental measurements of the temperature dependence of the H + O₂ reaction, in nitrogen moderator over a temperature range comparable to the present study, both of which reported negative “activation” energies, $-(6.9 \pm 1.1)$ kJ/mol⁵⁰ and $-(5.6 \pm 0.8)$ kJ/mol,^{48,49} resulting from fitting the data to the standard Arrhenius expression. An earlier measurement by Kurylo in He moderator gave a less negative value for the activation energy, $-(2.0 \pm 0.4)$ kJ/mol.⁴¹ Although seemingly difficult to justify theoretically, negative activation energies are usually explained as arising from exothermic preequilibria,¹⁰⁸ as in reactions R1 and R3 here. The room-temperature values for $k_{\text{ch}}^0(\text{H})$ from refs 50 and 48 and 49 just agree (Table 1); their values also agree, within errors, with a single measurement by Pratt and Wood at 425 K.⁴⁵ The temperature dependences of k_{ch}^0 for the reactions of Mu (Figure 7) and H with O₂ are compared in Figure 9. The recommended $T^{-1.8}$ dependence of Atkinson et al., shown as the solid line, is recommended only for the range of 200–600 K. Unfortunately, the recent H-atom data does not extend much below room temperature, and the earlier data of Kurylo at lower temperatures seems to have quite a different temperature dependence.⁴¹ Since the Mu data has been obtained down to 115 K, we may be in a more suitable position to distinguish between the two models. The lowest dotted line is a fit to the Mu data, assuming a temperature-independent rate; the longer dashed line is a theoretical prediction, discussed below. According to Cobos et al., the temperature dependence of the low-pressure limiting rate constant for the H + O₂ reaction is mainly dependent on the weak collision factor β_c ⁴⁶ which follows the approximate form⁷⁰

$$\frac{\beta_c}{1 - \sqrt{\beta_c}} \cong - \frac{\langle \Delta E \rangle}{F_E k_B T} \quad (18)$$

where $\langle \Delta E \rangle$ is the average amount of total (up + down) energy transferred in a collision. As long as $\langle \Delta E \rangle$ is not strongly temperature dependent,¹⁰⁹ which is seen in the fitted values for $\text{H} + \text{O}_2$ ⁴⁶ as well as in the case of some polyatomics,^{81,109} $\beta_c(T)$ is indeed found to be roughly proportional to $1/T$, for a variety of small molecules as well.¹⁰⁹ Atkinson et al. recommend $k_{\text{ch}}^0(\text{H})$ linear with $T^{-1.8}$.⁵¹ From Figures 7 and 9 (note the scale change), it is clear that there is essentially no temperature dependence in the $\text{Mu} + \text{O}_2$ reaction over the (115–463 K) range of the experimental points, in marked contrast to the dependence seen for the $\text{H} + \text{O}_2$ reaction. This can be explained by the larger zero-point energy barrier for the $\text{Mu} + \text{O}_2$ reaction, which counteracts the expected negative temperature dependence of T^{-n} , as verified by calculating $k_{\text{ch}}^{0,\text{SC}}$ (eq 9) for the two isotopes. This yields a theoretical isotope effect in the absence of temperature-dependent weak-collision factors. On the assumption still that eq 8 is valid, after multiplication by the recommended value for $k_{\text{ch}}^0(\text{H})$ of Atkinson et al.⁵¹ (the solid line in Figure 9 for $\text{H} + \text{O}_2$), the dependence for the $\text{Mu} + \text{O}_2$ reaction is obtained (long dashes in Figure 9). Such a calculation reproduces qualitatively the temperature dependence in the $\text{Mu} + \text{O}_2$ experimental data, even though the magnitude of the predicted KIE at room temperature is too small. This discrepancy is getting smaller when $\beta_c(\text{Mu}) = 1/2\beta_c(\text{H})$ is assumed (dash-dotted line in Figure 9). The trend would in fact be better reproduced if the lowest T point at 115 K were ignored, which may be justified by the fact that the $T^{-1.8}$ dependence of ref 51 is not warranted at low temperatures. Regardless, it is clear that the temperature dependence in $k_{\text{ch}}^0(\text{Mu})$ is far different from that of $\text{H} + \text{O}_2$ data, another manifestation of the sensitivity of the light-atom Mu mass to the dynamics.

Finally, it is appropriate here to revisit the earlier-commented discrepancy in the values of $k_{\text{ch}}^0(\text{Mu})$ between the high-pressure data at room temperature (Figure 3), taken at the TRIUMF accelerator, and the low-pressure (2 bar) data at varying temperatures, taken at the PSI accelerator (Figures 7 and 9). These values differ by almost a factor of 2. We have assumed this to represent some level of systematic error of unknown origin, giving rise to the aforementioned average $(8.0 \pm 2.1) \times 10^{-33} \text{ cm}^6 \text{ s}^{-1}$, leading to the KIE already discussed of 0.15 ± 0.05 . On the other hand, it is also well-known from basic ideas of RRKM theory that, at least for activation processes, the rate constant can increase with decreasing pressure, since there is a preponderance of lower-excitation molecules which have not been deactivated by collisions. This could mean a relatively smaller value for k_{ch}^0 at high pressures, consistent with the values seen here, but this can only be confirmed by further experiments of the temperature dependence of the $\text{Mu} + \text{O}_2$ reaction at high pressures (and/or rigorous theoretical calculations).

V. Concluding Remarks

We have investigated the recombination reaction of the remarkably light hydrogen isotope muonium with oxygen in N_2 moderator by applying the longitudinal field time differential μSR technique. The accuracy of the rate constant obtained with this method is similar to that obtained with conventional methods. At the lowest pressure, 2 bar, no temperature dependence was observed in the range from 115 to 463 K. The moderator (N_2) pressure dependence was investigated at room temperature, up to 301 bar. The overall bimolecular chemical

rate constant (k_{ch}) depends linearly on the moderator concentration over the entire pressure range, within the error limits of the experiments. The average termolecular low-pressure limiting rate constant is found to be $k_{\text{ch}}^0(\text{Mu}) = (8.0 \pm 2.1) \times 10^{-33} \text{ cm}^6 \text{ s}^{-1}$ and corresponds to a strong “inverse” kinetic isotope effect, $k_{\text{ch}}^0(\text{Mu})/k_{\text{ch}}^0(\text{H}) \approx 0.15$, in comparison with the analogous $\text{H} + \text{O}_2$ reaction.⁵¹ This experimental result provides the basis for an important test of the theories of $\text{H}(\text{Mu}) + \text{O}_2$ recombination kinetics, exploiting the unusual mass sensitivity afforded by studies of Mu reactivity. The principal theoretical formalism we have utilized in interpreting the experimental results is that of Troe,^{70–80} with a Morse-type potential for the $\text{Mu}(\text{H}) + \text{O}_2$ interaction. The calculated KIE with this formalism is 0.42 at room temperature, assuming no isotope effect in the weak collision factor, $\beta_c(\text{Mu}) = \beta_c(\text{H})$, in qualitative agreement with the experimental results. With the same assumption and adopting the $T^{-1.8}$ dependence that accounts for the H-atom data,⁵¹ the lack of any strong temperature dependence in the Mu reaction, which is in marked contrast to that observed for $\text{H} + \text{O}_2$ (Figure 9), can also be accounted for qualitatively.

Despite the relative success of Troe’s theory in accounting for the experimental $\text{Mu}(\text{H}) + \text{O}_2$ rate constants, the discrepancies revealed by the present study also raise questions about the validity of some of the approximations, in particular for the present system. There are mainly three points which are of concern. (i) The theory used here is based primarily on concepts of thermal distribution functions and, while nonequilibrium effects are in principle accounted for, it is not clear that this can be justified with the same degree of confidence for the markedly reduced density of states expected for the Mu atom analogue. (ii) The usual formulations and formulas are either based on approximations or are used in an approximate form, and it is not clear what the cumulative effect of these approximations is. To assess this question, it is first of all necessary to replace the presently used Morse potential and repeat the calculations based on the most reliable potential energy surface. Such work using the surface of Pastrana⁸⁹ is currently underway.⁹⁶ (iii) Perhaps most importantly, the SACM formalism is a semiclassical one which includes quantum effects in zero-point energies and in partition functions over discrete states, but it does not account for further nonclassical effects. The quantum fluctuations seen in the dissociation of HO_2^* ^{31,32,35} can be expected to be much more dramatic for MuO_2^* , with an average lifetime likely different from the RRKM average. Moreover, even though $\text{H} + \text{O}_2$ is believed to be a zero electronic barrier reaction, tunneling through the centrifugal barrier could effect the individual rate constants and discriminate further between Mu and H . It is hoped that the present study will motivate rigorous quantum calculations of the $\text{Mu} + \text{O}_2$ and $\text{H} + \text{O}_2$ reaction rates.

Acknowledgment. Support by the accelerator staff and the μSR facility groups at TRIUMF and at PSI are gratefully acknowledged, and D. G. Fleming acknowledges the financial support provided by NSERC (Canada).

References and Notes

- (1) Walker, D. C. *J. Chem. Phys.* **1981**, *85*, 3960.
- (2) Roduner, E.; Louwrier, P. W. F.; Brinkman, G. A.; Garner, D. M.; Reid, I. D.; Arseneau, D. J.; Senba, M.; Fleming, D. G. *Ber. Bunsen-Ges. Phys. Chem.* **1990**, *94*, 1224.
- (3) Baer, S.; Fleming, D. G.; Senba, M.; Gonzalez, A. In *Isotope Effects in Gas-Phase Chemistry*; Adv. Chem. Ser. 502; American Chemical Society: Washington, DC, 1992; Chapter 11.

- (4) Reid, I. D.; Garner, D. M.; Lap, Y. L.; Senba, M.; Arseneau, D. J.; Fleming, D. G. *J. Phys. Chem.* **1987**, *86*, 5578.
- (5) Snooks, R.; Arseneau, D. J.; Baer, S.; Fleming, D. G.; Senba, M.; Pan, J. J.; Shelley, M. *Hyperfine Interact.* **1994**, *87*, 911.
- (6) Roduner, E. *Prog. React. Kinet.* **1986**, *14*, 1.
- (7) Gonzalez, A. C.; Reid, I. D.; Garner, D. M.; Senba, M.; Fleming, D. G.; Arseneau, D. J.; Kempton, J. R. *J. Chem. Phys.* **1989**, *91*, 6164.
- (8) Takayanagi, T.; Kurosaki, Y. *J. Phys. Chem. A* **1997**, *101*, 7098.
- (9) Gonzalez, A. C.; Tempelmann, A.; Arseneau, D. J.; Fleming, D. G.; Senba, M.; Kempton, J. R.; Pan, J. J. *J. Chem. Phys.* **1992**, *97*, 6309.
- (10) Lynch, G. C.; Truhlar, D. G.; Brown, F. B.; Zhao, J.-G. *J. Phys. Chem.* **1995**, *99*, 207.
- (11) Lynch, G. C.; Truhlar, D. G.; Brown, F. B.; Zhao, J.-G. *Hyperfine Interact.* **1994**, *87*, 885.
- (12) Pan, J. J.; Arseneau, D. J.; Senba, M.; Shelley, M.; Fleming, D. G. *J. Phys. Chem.* **1997**, *101*, 8470.
- (13) Garner, D. M.; Fleming, D. G.; Arseneau, D. J.; Senba, M.; Reid, I. D.; Mikula, R. J. *J. Chem. Phys.* **1990**, *93*, 1732.
- (14) Duchovic, R. J.; Wagner, A. F.; Turner, E.; Garner, D. M.; Fleming, D. G. *J. Chem. Phys.* **1991**, *94*, 2794.
- (15) Roduner, E.; Münger, K. *Hyperfine Interact.* **1990**, *17*, 793.
- (16) Burkhard, P.; Roduner, E.; Hochmann, J.; Fischer, H. *J. Phys. Chem.* **1984**, *88*, 773.
- (17) Dilger, H.; Schwager, M.; Tregenna-Piggott, P. L. W.; Roduner, E.; Reid, I. D.; Arseneau, D. J.; Pan, J. J.; Senba, M.; Shelley, M.; Fleming, D. G. *J. Phys. Chem.* **1996**, *100*, 6561.
- (18) Dilger, H.; Stolmar, M.; Himmer, U.; Roduner, E.; Reid, I. D. *J. Phys. Chem. A* **1998**, *102*, 6772.
- (19) Ahumada, J. J.; Michael, J. V.; Osborne, D. T. *J. Chem. Phys.* **1972**, *57*, 3736.
- (20) Jachimowski, C. J. In *Major Research Topics in Combustion*; Hussaini, M., Kumar, A., Voit, R., Eds.; Springer-Verlag: New York, 1992; pp 339–358.
- (21) Miller, J. A.; Kee, R. J.; Westbrook, C. *Annu. Rev. Phys. Chem.* **1990**, *41*, 345.
- (22) Miller, J. A. *J. Chem. Phys.* **1986**, *84*, 6170.
- (23) Pan, J. J.; Senba, M.; Arseneau, D. J.; Gonzales, A. C.; Kempton, J. R.; Fleming, D. G. *J. Phys. Chem.* **1995**, *99*, 17160.
- (24) Hartley, D. B.; Thrush, B. A. *Proc. R. Soc. London, Ser. A* **1967**, *297*, 520.
- (25) Arseneau, D. J.; Pan, J. J.; Senba, M.; Shelley, M.; Fleming, D. G. *Hyperfine Interact.* **1997**, *106*, 151.
- (26) Lielievold, J.; Crutzen, P. *J. Nature* **1990**, *343*, 227.
- (27) Warnatz, J. In *Combustion Chemistry*; Gardiner, W. C., Ed.; Springer-Verlag: New York, 1984; p 197.
- (28) Dai, J.; Zhang, J. Z. H. *J. Phys. Chem.* **1996**, *100*, 3664.
- (29) Zhang, D.; Zhang, J. Z. H. *J. Phys. Chem.* **1994**, *101*, 3671.
- (30) Song, K.; Peslherbe, G. H.; Hase, W. L.; Dobbyn, A. J.; Stumpf, M.; Schinke, R. *J. Chem. Phys.* **1995**, *103*, 8891.
- (31) Dobbyn, A. J.; Stumpf, M.; Keller, H.-M.; Schinke, R. *J. Chem. Phys.* **1996**, *104*, 8357.
- (32) Dobbyn, A. J.; Stumpf, M.; Keller, H.-M.; Hase, W. L.; Schinke, R. *J. Chem. Phys.* **1995**, *102*, 5867.
- (33) Kendrick, B.; Pack, R. T. *J. Chem. Phys.* **1996**, *104*, 7475.
- (34) Kendrick, B.; Pack, R. T. *J. Chem. Phys.* **1996**, *104*, 7502.
- (35) Mandelshtam, V. A.; Taylor, H. S.; Miller, W. H. *J. Chem. Phys.* **1996**, *105*, 496.
- (36) Duchovic, R. J.; Pettigrew, J. D.; Welling, B.; Shipchandler, T. *J. Chem. Phys.* **1996**, *105*, 10367.
- (37) Duchovic, R. J.; Pettigrew, J. D. *J. Phys. Chem.* **1994**, *98*, 10794.
- (38) Yuan, T.; Wang, C.; Yu, C.-L.; Frenklach, M.; Rabinowitz, M. *J. Phys. Chem.* **1991**, *95*, 1258.
- (39) Kessler, K.; Kleinermanns, K. *J. Chem. Phys.* **1992**, *97*, 374.
- (40) Bronikowski, M. J.; Zhang, R.; Rakestraw, D. J.; Zare, R. N. *Chem. Phys. Lett.* **1989**, *156*, 7.
- (41) Kurylo, M. J. *J. Phys. Chem.* **1972**, *76*, 3518.
- (42) Wong, W.; Davis, D. D. *Int. J. Chem. Kinet.* **1974**, *1*, 401.
- (43) Hack, W.; Wagner, H. Gg.; Hoyermann, K. *Ber. Bunsen-Ges. Phys. Chem.* **1978**, *82*, 713.
- (44) Campbell, I. M.; Rogerson, J. S.; Handy, B. J. *Faraday Trans. 1* **1978**, *11*, 2672.
- (45) Pratt, G. L.; Wood, S. W. *J. Chem. Soc., Faraday Trans.* **1983**, *79*, 2597.
- (46) Cobos, C. J.; Hippler, H.; Troe, J. *J. Phys. Chem.* **1985**, *89*, 342.
- (47) Pirraglia, A. N.; Michael, J. V.; Sutherland, J. W.; Klemm, R. B. *J. Phys. Chem.* **1989**, *93*, 282.
- (48) Hsu, K.-J.; Anderson, S. M.; Durant, J. L.; Kaufman, F. *J. Phys. Chem.* **1989**, *93*, 1018.
- (49) Hsu, K.-J.; Durant, J. L.; Kaufmann F. *J. Phys. Chem.* **1987**, *91*, 1895.
- (50) Carleton, K. L.; Kessler, W. J.; Marinelli, W. J. *J. Phys. Chem.* **1993**, *97*, 6412.
- (51) Atkinson, R.; Baulch, D. L.; Cox, R. A.; Hampson, R. F., Jr.; Kerr, J. A.; Rossi, M. J.; Troe, J. *J. Phys. Chem. Ref. Data* **1997**, *26* (3), 521.
- (52) Breshears, W. D.; Fry, H. A.; Shea, R. F.; Wilson, C. W. *J. Chem. Soc., Faraday Trans.* **1991**, *87*, 2337.
- (53) Fleming, D. G.; Senba, M. In *Perspectives of Meson Science*; Yamazaki, T., Nakai, K., Nagamine, K., Eds.; North-Holland: Amsterdam, 1992; pp 219–264.
- (54) Roduner, E. *Chem. Soc. Rev.* **1993**, *22*, 337.
- (55) Roduner, E. *The Positive Muon as a Probe in Free Radical Chemistry*; Lecture Notes in Chemistry 49; Springer-Verlag: Berlin, 1988.
- (56) Roduner, E. *App. Magn. Reson.* **1997**, *13*, 1.
- (57) Senba, M.; Gonzales, A. C.; Kempton, J. R.; Arseneau, D. J.; Pan, J. J.; Tempelmann, A.; Fleming, D. G. *Hyperfine Interact.* **1990**, *65*, 979.
- (58) D'Ans-Lax *Taschenbuch für Physiker und Chemiker*, 4th ed.; Blachnik, R., Ed.; Springer: Berlin, 1998; Vol. 3, p 1040.
- (59) James, F.; Roos, M. *Comput. Phys. Commun.* **1975**, *10*, 343. James, F.; *MINUIT Reference Manual*; CERN, 1994.
- (60) Pan, J. J. Ph.D. Thesis, University of British Columbia, Vancouver, BC, 1995.
- (61) Fleming, D. G.; Pan, J. J.; Senba, M.; Arseneau, D. J.; Kiefl, R. F.; Shelley, M. *J. Phys. Chem.* **1996**, *100*, 7517.
- (62) Dilger, H.; Roduner, E.; Stolmar, M.; Reid, I. D.; Fleming, D. G.; Arseneau, D. J.; Pan, J. J.; Senba, M.; Shelley, M. *Hyperfine Interact.* **1997**, *106*, 137.
- (63) Brewer, J. H.; Crowe, K. M.; Gygas, F. N.; Schenck, A. In *Muon Physics*; Hughes, V. W., Wu, C. S., Eds.; Academic Press: New York, 1975; Vol. III, Chapter VII.
- (64) Turner, R. E.; Snider, R. F.; Fleming, D. G. *Phys. Rev. A* **1990**, *41*, 1505.
- (65) Weltner, W. *Magnetic Atoms and Molecules*; Dover Publications: New York, 1982; Table D-4.
- (66) Pan, J. J.; Fleming, D. G.; Senba, M.; Arseneau, D. J.; Snooks, R.; Baer, S.; Shelley, M.; Percival, P. W.; Brodovitch, J. C.; Addison-Jones, B.; Wlodek, S.; Cox, S. F. *J. Hyperfine Interact.* **1994**, *87*, 865.
- (67) Senba, M.; Fleming, D. G.; Arseneau, D. J.; Garner, D. M.; Reid, I. D. *Phys. Rev. A* **1989**, *39*, 3871.
- (68) Stallcop, J. R.; Partridge, H.; Levin, E. *Phys. Rev. A* **1996**, *53*, 766.
- (69) Baulch, D. L.; Cobos, C. J.; Cox, R. A.; Esser, C.; Frank, P.; Just, Th.; Kerr, J. A.; Pilling, M. J.; Troe, J.; Walker, R. W.; Warnatz, J. *J. Phys. Chem. Ref. Data* **1992**, *21*, 411.
- (70) Troe, J. *J. Chem. Phys.* **1977**, *66*, 4745.
- (71) Troe, J. *J. Chem. Phys.* **1977**, *66*, 4758.
- (72) Troe, J. *J. Phys. Chem.* **1979**, *83*, 114.
- (73) Troe, J. *J. Chem. Phys.* **1981**, *75*, 226.
- (74) Troe, J. *Ber. Bunsen-Ges. Phys. Chem.* **1983**, *87*, 161.
- (75) Troe, J. *Ber. Bunsen-Ges. Phys. Chem.* **1983**, *87*, 169.
- (76) Troe, J. *J. Chem. Phys.* **1983**, *79*, 6017.
- (77) Troe, J. *J. Chem. Phys.* **1992**, *97*, 288.
- (78) Troe, J. *Ber. Bunsen-Ges. Phys. Chem.* **1994**, *98*, 1399.
- (79) Troe, J. *Annu. Rev. Phys. Chem.* **1978**, *29*, 223.
- (80) Troe, J. In *Physical Chemistry: an Advanced Treatise*; Eyring, H., Henderson, D., Jost, W., Eds.; Academic: New York, 1975; Vol. VIB Press, Chapter 11.
- (81) Seakins, P. W.; Robertson, S. H.; Pilling, M. J.; Slagle, I. R.; Gmurczyk, G. W.; Bencsura, A.; Gutman, D.; Tsang, W. *J. Phys. Chem.* **1993**, *97*, 4450.
- (82) Ahlrichs, R.; Bär, M.; Häser, M.; Horn, H.; Kölmel, C. *Chem. Phys. Lett.* **1989**, *162*, 165.
- (83) Becke, A. D. *Phys. Rev. A* **1988**, *38*, 3098.
- (84) Lee, C.; Yang, W.; Parr, R. G. *Phys. Rev. B* **1988**, *37*, 785.
- (85) Roduner, E.; Reid, I. D. *Israel J. Chem.* **1989**, *29*, 3.
- (86) Walch, S. P.; Duchovic, R. J. *J. Chem. Phys.* **1991**, *94*, 7068.
- (87) Walch, S. P.; Rohlfing, C. M. *J. Chem. Phys.* **1989**, *91*, 2373.
- (88) Walch, S. P.; Rohlfing, C. M.; Melius, C. F.; Bauschlicher, C. W. *J. Chem. Phys.* **1988**, *88*, 6273.
- (89) Pastrana, M. R.; Quintales, L. A. M.; Brandão, J.; Varandas, A. J. C. *J. Phys. Chem.* **1990**, *94*, 8073.
- (90) Mar, P. L.; Katrina, S.; Werpinski, M. C. *Chem. Phys. Lett.* **1998**, *287*, 195.
- (91) Melius, C. F.; Blint, R. J. *Chem. Phys. Lett.* **1979**, *64*, 183.
- (92) Yang, Y.-C.; Klippenstein, S. J. *J. Chem. Phys.* **1995**, *103*, 7287.
- (93) Varandas, A. J. C. *J. Chem. Phys.* **1993**, *99*, 1076.
- (94) Varandas, A. J. C.; Brandao, J.; Pastrana, M. R. *J. Chem. Phys.* **1992**, *96*, 5137.
- (95) Leforestier, C.; Miller, W. H. *J. Chem. Phys.* **1994**, *100*, 733.
- (96) Himmer, U.; Roduner, E. To be published.
- (97) Main, J.; Jung, C.; Taylor, H. S. *J. Chem. Phys.* **1997**, *107*, 6577.
- (98) Toselli, B. M.; Barker, J. R. *J. Chem. Phys.* **1992**, *97*, 1809.
- (99) Mehlmann, C.; Frost, M. J.; Heard, D. E.; Orr, B. J.; Nelson, P. F. *J. Chem. Soc., Faraday Trans.* **1996**, *92*, 2395.
- (100) Dashevskaya, E. I.; Nikitin, E. E.; Troe, J. *J. Chem. Phys.* **1992**, *97*, 3318.
- (101) Lendvay, G. *J. Phys. Chem. A* **1997**, *101*, 9217.

- (102) Lendvay, G. Personal communication.
- (103) Guadagnini, R.; Schatz, G. C.; Walch, S. P. *J. Chem. Phys.* **1995**, *102* (2), 774.
- (104) Guadagnini, R.; Schatz, G. C.; Walch, S. P. *J. Chem. Phys.* **1995**, *102* (2), 784.
- (105) Pan, J. J.; Arseneau, D. J.; Himmer, U. et al. In preparation.
- (106) Cobos, C. J.; Troe, J. *J. Chem. Phys.* **1983**, *83*, 1010.
- (107) Prezhdo, O. *J. Phys. Chem.* **1995**, *99*, 8633.
- (108) Fontijn, A.; Zellner, R. In *Reactions of Small Transient Species, Kinetics and Energetics*; Fontijn, A., Clyne, M. A. A., Eds., Academic: New York, 1983; Chapter 1.
- (109) Luther, K.; Troe, J. In *Reactions of Small Transient Species, Kinetics and Energetics*; Fontijn, A., Clyne, M. A. A., Eds.; Academic: New York, 1983; Chapter 2.